THE JOURNAL OF BIOLOGICAL CHEMISTRY VOL. 286, NO. 11, pp. 9477–9488, March 18, 2011

Identification of SPRED2 (Sprouty-related Protein with EVH1 Domain 2) as a Negative Regulator of the Hypothalamic-Pituitary-Adrenal Axis*

Received for publication, August 2, 2010, and in revised form, December 22, 2010 Published, JBC Papers in Press, January 3, 2011, DOI 10.1074/jbc.M110.171306

Melanie Ullrich[‡1], Karin Bundschu[§], Peter M. Benz[‡], Marco Abesser[‡], Ruth Freudinger[‡], Tobias Fischer[‡], Julia Ullrich[‡], Thomas Renné[¶], Ulrich Walter[‖], and Kai Schuh[‡2]

From the [‡]Institute of Physiology I, University of Wuerzburg, Roentgenring 9, 97070 Wuerzburg, Germany, the [§]Institute of Biochemistry and Molecular Biology, University of Ulm, Albert-Einstein-Allee 11, 89081 Ulm, Germany, the [¶]Department of Molecular Medicine and Surgery, Karolinska Institutet, Karolinska University Hospital Solna, SE-17176 Stockholm, Sweden, and the [‖]Institute of Clinical Biochemistry and Pathobiochemistry, University of Wuerzburg, Oberduerrbacher Strasse 6, 97080 Wuerzburg, Germany

Sprouty-related proteins with EVH1 (enabled/vasodilator-stimulated phosphoprotein homology 1) domain (SPREDs) are inhibitors of MAPK signaling. To elucidate SPRED2 *in vivo* function, we characterized body homeostasis in SPRED2$^{-/-}$ mice. They showed a doubled daily water uptake, induced by elevated serum osmolality, originating from increased blood salt load. Accordingly, serum aldosterone was doubled, accompanied by augmented adrenal aldosterone synthase (AS) expression. Surprisingly, serum vasopressin (AVP) was unaltered, and, as evidenced by halved angiotensin II (Ang II) levels, the renin angiotensin system (RAS) was down-regulated. Adrenocorticotropic hormone (ACTH) was significantly elevated in SPRED2$^{-/-}$ mice, together with its secretagogue corticotropin-releasing hormone (CRH) and its downstream target corticosterone. ERK phosphorylation in brains was augmented, and hypothalamic CRH mRNA levels were elevated, both contributing to the increased CRH release. Our data were supported by CRH promoter reporter assays in hypothalamic mHypoE-44 cells, revealing a SPRED-dependent inhibition of Ets (ERK/E-twenty-six)-dependent transcription. Furthermore, SPRED suppressed CRH production in these cells. In conclusion, our study suggests that SPRED2 deficiency leads to an increased MAPK signaling, which results in an augmented CRH promoter activity. The subsequent CRH overproduction causes an up-regulation of downstream hypothalamic-pituitary-adrenal (HPA) hormone secretion. This constitutes a possible trigger for the observed compulsive grooming in SPRED2$^{-/-}$ mice and may, together with hyperplasia of aldosterone-producing cells, contribute to the hyperaldosteronism and homeostatic imbalances.

The HPA[3] axis is essential to maintain homeostasis and to manage physical or emotional stress. It comprises a complex set of direct and feedback interactions among the hypothalamus, the pituitary, and the adrenal glands. Triggered by the limbic system, activation of the HPA axis begins with hypothalamic release of CRH (1). Secreted into the portal pituitary circulation, it there stimulates the secretion of the proopiomelanocortin cleavage product ACTH by the anterior pituitary (2, 3). CRH-induced ACTH release regulates the secretion of various hormones of the adrenal gland cortex (*e.g.* the mineralocorticoid aldosterone, glucocorticoids like cortisol and corticosterone, and androgens) (4, 5). The stress hormones cortisol and corticosterone, respectively, act as important negative feedback regulators of the HPA axis by exerting a long feedback loop to the hypothalamus and a short loop to the pituitary. CRH inhibition by ACTH also represents a short negative feedback loop (4, 6). Dysregulation of the HPA axis plays a fundamental role in stress-associated pathologies, mood, neurodegenerative disorders, and anxiety (7, 8). AVP, a major regulator of renal water reabsorption, is produced in hypothalamus and released from posterior pituitary in response to hyperosmolality or hypovolemia. It exerts its antidiuretic effects by triggering the insertion of AQP2 (aquaporin-2) water channels into the luminal membrane of collecting duct principle cells (9, 10). Aldosterone is another potent regulator of extracellular fluid and salt balances by promoting Na^+ retention and K^+ secretion in the distal nephron of the kidney. Aldosterone release from the adrenal cortex is mainly stimulated by K^+, the RAS, and ACTH (11). The critical enzyme in the late pathway of aldosterone biosynthesis is the AS, an enzyme primarily expressed in adrenal zona glomerulosa cells (12, 13). Dysregulation of aldosterone secretion is causally involved in diseases like arterial hypertension, cardiac fibrosis, cardiovascular dysfunction, and progressive renal disease (14). HPA hormone actions are mainly mediated

* This work was supported by Deutsche Forschungsgemeinschaft Grant SCHU1600/2-1 (to K. S.) and a grant from the Stiftung fuer Pathobiochemie und Molekulare Diagnostik of the Deutsche Vereinte Gesellschaft fuer Klinische Chemie und Laboratoriumsmedizin e.V. (to K. S. and U. W.).

[1] To whom correspondence may be addressed. Tel.: 49-931-31-80133; Fax: 49-931-31-82741; E-mail: m.ullrich@uni-wuerzburg.de.

[2] To whom correspondence may be addressed. Tel.: 49-931-31-82740; Fax: 49-931-31-82741; E-mail: kai.schuh@uni-wuerzburg.de.

[3] The abbreviations used are: HPA, hypothalamic-pituitary-adrenal; ACTH, adrenocorticotropic hormone; Ang II, angiotensin II; AQP, aquaporin; AS, aldosterone synthase; AVP, arginine vasopressin; b-geo, b-galactosidase-neomycin phosphotransferase; CK, creatine kinase; CRH, corticotropin-releasing hormone; Ets, ERK/E-twenty six; EVH1, enabled/vasodilator-stimulated phospoprotein homology 1; GGT, γ-glutamyltransferase; GH, growth hormone; GOT/AST, glutamate oxaloacetate transaminase/aspartate aminotransferase; GPT/ALT, glutamate pyruvate transaminase/alanine aminotransferase; HET, heterozygous; IGF, insulin-like growth factor 1; KBD, c-Kit binding domain; PVN, paraventricular nucleus; RAS, renin-angiotensin system; SPR domain, Sprouty-like domain; SPRED, Sprouty-related protein with EVH1 domain.

by G protein-coupled and steroid receptors. To date, only first insights have been obtained into how receptor tyrosine kinases and MAPKs participate in the regulation of the HPA axis (15–18).

SPRED proteins are membrane-associated suppressors of MAPK signaling, a major regulator of cellular proliferation and differentiation. Pathway activation results in phosphorylation of transcription factors (*e.g.* Ets factors) and other target proteins (19, 20). So far, three mammalian SPRED isoforms were described, and additional splice variants may exist (21, 22). SPRED2 contains an N-terminal EVH1 domain, a central c-Kit-binding domain (KBD), and a C-terminal cysteine-rich Sprouty-like (SPR) domain (21, 23). Both EVH1 and SPR domains are required for efficient suppression of MAPK signaling because deletion mutants lacking either the EVH1 or the SPR domain were unable to block growth factor-induced ERK activation (24). In summary, SPREDs are regarded as potent inhibitors of a wide range of mitogenic stimuli like growth factors, cytokines, and chemokines, but the suppressing effect seems to be restricted to the Ras/ERK/MAPK pathway (23–25). To date, promoter, RNA, and protein expression studies have revealed profound SPRED2 expression in neural and various glandular tissues and in kidney (26, 27). The first studies using SPRED1$^{-/-}$ and SPRED2$^{-/-}$ mice revealed that SPREDs are not essential for survival (28, 29) but play a role in hematopoiesis (25, 29, 30), and SPRED2 seems to be an important modulator of bone morphogenesis by inhibiting the fibroblast growth factor-induced MAPK pathway (28). Interestingly, a similar phenotype was also mentioned for SPRED1$^{-/-}$ mice (29, 31), underlining the role of SPRED proteins in growth regulation and supporting the idea of overlapping physiological functions. In agreement, SPRED1/2 double-deficient mice suffer from embryonic lethality due to impaired lymphogenesis, causing fatal hemorrhage (32). *Spred1* loss-of-function mutations in humans cause the neurofibromatosis type 1-like Legius syndrome, characterized by café-au-lait spots, axillary freckling, facial abnormalities, and behavioral and learning problems but lacking neurofibromas (31, 33–35). Similarly, SPRED1$^{-/-}$ mice develop facial abnormalities and show impaired hippocampus-dependent learning (31, 36). In addition, SPRED1 knockdown studies in mice underlined its importance for brain development and supported the hypothesis of its involvement in vesicle transport (26, 37).

Based on the observation of obsessive grooming, abnormal water uptake, and signs of homeostatic imbalances, we searched for a common elicitor causing this versatile phenotype. Increased aldosterone levels and AS expression in SPRED2$^{-/-}$ mice provoked an elevated blood salt load and hyperosmolality, the latter contributing to the polydipsia. HPA hormone secretion was completely up-regulated, as confirmed by significantly increased CRH, ACTH, and corticosterone levels. Due to the missing inhibition of MAPK signaling, ERK phosphorylation was elevated in brains of SPRED2$^{-/-}$ mice, and hypothalamic CRH mRNA content was higher. *In vitro* assays in mHypoE-44 cells with CRH promoter and 4xEts firefly luciferase reporters revealed SPRED-dependent inhibition of CRH transcription. In addition, transient SPRED expression suppressed CRH secretion of these cells. In summary, SPRED2 deficiency causes an augmented secretion of CRH and of CRH-dependent HPA hormones. HPA overactivation might provide a prevalent reason for compulsive grooming, and, in combination with elevated adrenal AS expression, this might be involved in the development of hyperaldosteronism. Thus, we present a new link between HPA axis regulation and SPRED-dependent MAPK/ERK/Ets pathway inhibition.

EXPERIMENTAL PROCEDURES

Animals—SPRED2$^{-/-}$ mice were generated by blastocyst injection of the embryonic stem cell line XB228 (International Gene Trap Consortium) (28). SPRED2$^{-/-}$ mice were obtained by mating SPRED2$^{+/-}$ animals, and their SPRED2$^{+/+}$ littermates were used as controls. To minimize possible inbred effects, mice were raised on a mixed 129/Ola × C57Bl/6 genetic background. Mice were kept in plastic cages on a daily 12-h light/dark cycle with a room temperature of 25 °C, humidity of 50%, and tap water and standard mouse chow *ad libitum* unless stated otherwise. All experiments were approved by the local councils for animal care and were conducted according to the European law for animal care and use.

Examination of Water Uptake—Mice were kept separately under standard conditions. Water consumption was recorded each day over a period of 1 month, and the average daily water uptake was calculated in relation to body weight.

Water Deprivation Experiment—Mice were kept under standard conditions but water-starved for 48 h while having free access to mouse chow. Control and water-deprived mice were weighed, and serum osmolalities were determined via freezing point depression (Osmomat 030, Gonotec). For organ/body weight ratios, total weights of brains, adrenal glands, and kidneys were measured individually and related to the corresponding body weights.

Determination of Serum Parameters and Hormone Levels—For routine laboratory measurements, mice were anesthetized by intraperitoneal injection of avertin (tribromethanol, 250 mg/kg body weight), blood was collected from the retro-orbital plexus, and clotted in serum tubes (Sarstedt) for 1 h. After centrifugation at 10,000 × *g* for 3 min, the parameters summarized in Table 1 were determined from serum supernatant using established and quality-controlled methods by standard automated laboratory analyzers in the Central Core Laboratory of the University Hospital Wuerzburg. To measure serum Ang II, aldosterone, ACTH, corticosterone, GH, and IGF-1, blood was collected from avertin-anesthetized mice between 9 and 12 a.m., and sera were prepared as described above. Serum samples were stabilized with Complete protease inhibitor mixture (Roche Applied Science), aliquoted, and stored at −80 °C. Measurements of hormone levels were performed by enzyme immunoassay or ELISA using commercially available assays: aldosterone (ALPCO Diagnostics), corticosterone (Diagnostic Systems Laboratories, Inc.), ACTH and Ang II (Peninsula Laboratories, LLC), growth hormone (Millipore), and IGF-1 (Assay Pro). For determination of serum AVP by enzyme immunoassay (Assay Designs), water-starved and non-starved mice were decapitated between 1 and 4 p.m. Trunk blood was collected, and serum was prepared, aliquoted, and frozen as described above. In cell culture supernatants of mock- or SPRED-trans-

fected mHypoE-44 cells and PVN-containing brain lysates, CRH was estimated by ELISA (Yanaihara Institute Inc.). Cell culture supernatants were taken after 48 h of starvation in low glucose DMEM (1 g/liter) without FBS. Hypothalamus lysates were stabilized by Complete protease inhibitor mixture (Roche Applied Science), aliquoted, and stored at −80 °C. Hormonal concentrations were calculated from a standard curve using nonlinear regression curve fitting (Prism 4, GraphPad Software).

Cloning of EVH1-β-geo Fusion Protein and β-geo Expression Plasmids—RNA was extracted from brains of SPRED2 KO mice using TRIzol reagent (Invitrogen). 2 μg of total RNA was reverse transcribed and amplified with the Verso 1-Step RT-PCR kit (Thermo Scientific) using the following primers: NotI-S2-forward (for EVH1-β-geo), 5′-TAGCGGCCGCATGACCGAAGAAACACACCCGG-3′; NotI-β-geo-forward (for β-geo), 5′-TAGCGGCCGCGTCCCAGGTCCCGAAAACCAAA-3′; and HindIII-reverse (for both), 5′-ATAAGCTTTCAGAAGAACTCGTCAAGAAGG-3′. Resulting cDNAs were cloned into the NotI/HindIII sites of pcDNA3.1(−)/Myc-His B vector (Invitrogen).

Cell Culture and Transfection—HEK293 cells were cultured in high glucose DMEM (4.5 g/liter) supplemented with 10% FBS at 37 °C and 5% CO_2. 24 h prior to transfection, cells were either seeded on 6-well plates for preparation of protein extracts and Western blot analysis or on 2-well chamber slides (Nunc) for X-Gal stainings and grown to 90% confluence. Cells were transiently transfected with Lipofectamine 2000 (Invitrogen) using pcDNA3.1(−)/Myc-His expression plasmids for SPRED2, EVH1-β-geo, and β-geo or empty vector as negative control. After 24 h, cells were washed with PBS and homogenized for Western blot or fixed for X-Gal staining. mHypoE-44 cells (Cedarlane) were cultured in high glucose DMEM supplemented with 10% FBS at 37 °C and 5% CO_2. 24 h before transfection, cells were seeded on 96-well plates, grown overnight to 90% confluence, and transfected with Lipofectamine 2000 (Invitrogen) for luciferase reporter assays or CRH ELISA.

Luciferase Reporter Assays—A 5.7-kb region of the 5′ CRH promoter sequence containing exon 1 was amplified from 129/Ola × C57Bl/6 genomic mouse DNA, using the following primers: XhoI-CRH-forward, 5′-CCGCTCGAGATGGCCTTTCCAAGGGTAATTC-3′; XhoI-CRH-reverse, 5′-CCGCTCGAGCTCCTCCCTTGGTAGGTGAGC-3′. The CRH promoter region was cloned into the pGL3-basic firefly luciferase reporter vector (Promega) and transiently co-transfected with a *Renilla* luciferase control reporter vector (pRL-TK, Promega) into mHypoE-44 cells. To stimulate CRH promoter activity, cells were starved in low glucose DMEM without FBS for 24 h. Firefly luciferase activity was determined either in the presence of co-transfected SPRED1 or SPRED2, both in the presence and absence of EVH1-β-geo. Signals were normalized to *Renilla* luciferase activity by the Dual-Glo System (Promega). Mean values of single CRH promoter reporter-transfected samples were set to 1, and mean values of co-transfected samples were expressed as *x*-fold of 1. Accordingly, a 4xEts-like factor binding site-containing luciferase reporter (38) was co-transfected into mHypoE-44 cells, and luciferase activity was determined as described above.

Western Blotting—After transfection, cells were lysed in 2% SDS in PBS supplemented with Complete protease inhibitor mixture and PhosSTOP phosphatase inhibitor mixture (Roche Applied Science). For mouse organ lysates, 50 mg of tissue was homogenized with an Ultra Turrax (IKA) in 1 ml of 2% SDS sample buffer. Proteins were separated by 8% SDS-PAGE under reducing conditions and electrotransferred to nitrocellulose membranes (Schleicher & Schuell) using semidry blotters (Biometra). Blots were probed using primary polyclonal antibodies raised in rabbits against SPRED2 (1:500) (28), β-gal (1:5,000; Abcam), p44/42 MAPK (1:2,000; Cell Signaling), and phospho-p44/42 MAPK (1:1,000; Cell Signaling), followed by a goat anti-rabbit horseradish peroxidase-conjugated secondary antibody (1:10,000; Jackson ImmunoResearch), all diluted in 5% nonfat dry milk in PBS supplemented with 0.05% Tween 20. ECL Plus Western blotting reagent (GE Healthcare) was used for signal detection.

Northern Blotting—Mice were decapitated, brains were removed, and the hypothalamic PVN region was prepared. RNA was isolated using TRIzol. Northern blotting was performed as described previously (28) using a mouse CRH cDNA probe.

Quantification of ERK Phosphorylation and CRH mRNA Levels—Western blot exposures were scanned, and Northern blots were exposed to image plates of a BAS-1500 system (Fujifilm). After conversion to TIFF files, band intensities were quantified using ImageJ software (National Institutes of Health). Data were calculated as ratios of phospho-ERK to total ERK or of CRH mRNA band intensities to total RNA, respectively. The mean value of WT samples was set to 1, and the mean value of KO samples was expressed as *x*-fold of WT.

Immunohistochemistry—Dissected brains, pituitary glands, and adrenal glands were embedded in Tissue-Tek OCT compound (Sakura) and snap-frozen in liquid nitrogen. 10-μm cryosections were cut using a CM1950 microtome (Leica). Specimens were fixed in 4% paraformaldehyde in PBS for 10 min, permeabilized with 0.2% Triton X-100 in PBS for 20 min, and blocked in 10% goat serum in PBS for 1 h. Overnight incubation with primary rabbit polyclonal anti-SPRED2 (1:50) (28) and anti-AS antibodies (1:50 (39)) was followed by incubation with secondary goat anti-rabbit antibodies conjugated to Alexa Flour 488 or 594 for 2 h (1:1,000; Molecular Probes). All antibody incubations were performed in 10% goat serum in PBS in a humidified chamber in the dark. Stained sections were investigated using an Eclipse E600 microscope equipped with a C1 confocal scanning head and 10- and 100-fold objectives (Nikon).

X-Gal Staining—X-Gal stainings were performed as described previously (27, 40). Whole organs were photographed by a Coolpix 995 digital camera (Nikon), and cells and tissue sections were photographed as described above.

Statistical Analyses—Results are expressed as mean ± S.D. Data sets were analyzed by two-sample *t* tests or Welch's tests, depending on the homogeneity of variances. Normal distribution of data was ensured using box and quantile-quantile plot analysis tools provided by Statistica (StatSoft). Values of $p < 0.05$ were considered as statistically significant.

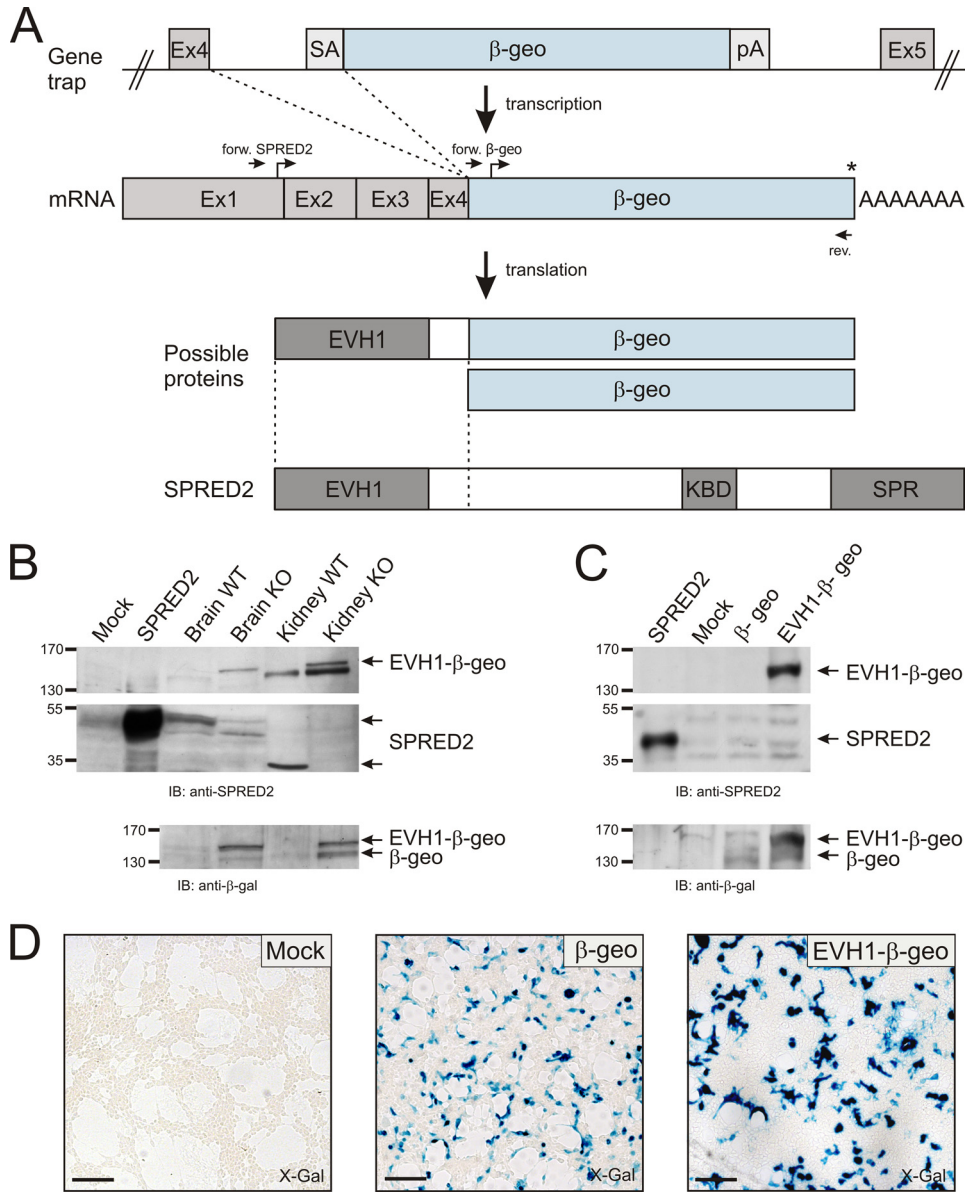

FIGURE 1. **Disruption of *Spred2* and expression of an EVH1-β-geo fusion protein in SPRED2$^{-/-}$ mice.** *A*, in SPRED2 KO mice, the *Spred2* gene was disrupted by insertion of a gene trap vector between exons 4 and 5. This vector contains a splice acceptor (*SA*), a reporter gene (β-geo) allowing expression profiling of the endogenous *Spred2* promoter via X-Gal stainings, and an SV40 polyadenylation sequence (*pA*). Upon transcription, β-geo is spliced to the end of exon 4 of *Spred2*, leading either to a fusion protein coding for the EVH1 domain of SPRED2 and the β-geo reporter, if protein translation starts at the start codon of *Spred2* exon1 (*first bent arrow*), or to the expression of β-geo alone, if translation starts at the start codon of β-geo (*second bent arrow*). In both cases, translation stops at the stop codon of β-geo (*). The *arrows* indicate the position of primers used to subclone EVH1-β-geo and β-geo. *B*, Western blots (*IB*) with tissue lysates analyzed with anti-SPRED2 (*top* and *middle*), and anti-β-gal antibodies (*bottom*) demonstrated SPRED2 expression in WT organs and the *in vivo* expression of both β-geo and EVH1-β-geo in SPRED2$^{-/-}$ mice. *C*, expression of EVH1-β-geo and β-geo in HEK293 cells after transfection with EVH1-β-geo and β-geo expression plasmids. Lysates were probed with anti-SPRED2 (*top* and *middle*) or anti-β-gal antibodies (*bottom*). *D*, X-Gal stainings of transfected HEK293 cells confirmed the enzymatic activity of the EVH1-β-geo fusion protein and β-geo. *Scale bars*, 100 μm.

RESULTS

SPRED2$^{-/-}$ Mice Are Functional Knockouts and Express an EVH1-β-geo Fusion Protein—To investigate the physiological consequences of SPRED deficiency, we used SPRED2 KO mice, which we generated by a gene trap approach as described earlier (28). In these KO mice, also used in this study, the *Spred2* gene was disrupted by insertion of a gene trap vector between exons 4 and 5 of *Spred2* (shown schematically in Fig. 1*A*). In this model, expression profiling can be monitored via enzymatic activity of the β-galactosidase-neomycin phosphotransferase fusion gene (β-geo), which came under control of the endogenous *Spred2* promoter. Although *Spred2* was interrupted by vector insertion, the first four exons of *Spred2*, mainly encoding the EVH1 domain, remained intact. Thus, upon transcriptional activation of the "trapped" *Spred2* gene, either a fusion protein harboring the EVH1 domain and β-geo or the sole β-geo reporter might be expressed. In order to examine if the EVH1-β-geo fusion protein was present in our SPRED2-deficient mice, we performed Western blot analysis using either an anti-SPRED2 antibody, which recognizes an epitope in the coding sequence of exon 4 (28), or an anti-β-gal antibody (Fig. 1*A*). Anti-SPRED2 antibodies detected the common 46-kDa

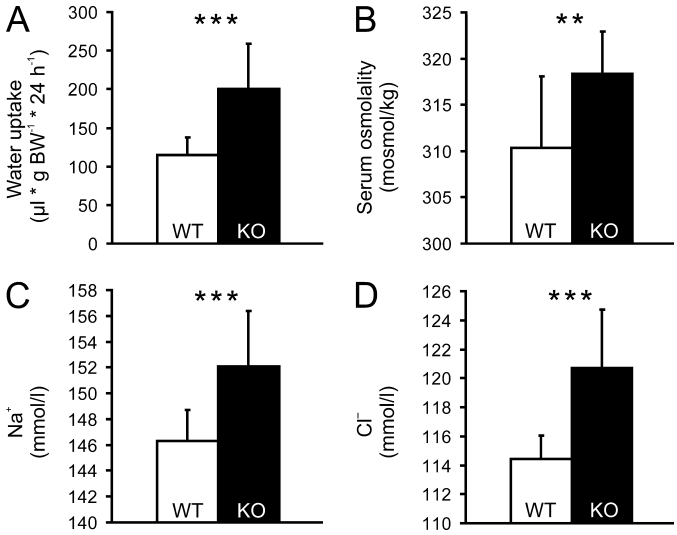

FIGURE 2. **Excessive water uptake correlates with elevated serum osmolality and increased salt concentrations.** *A*, nearly doubled daily water consumption in KO mice. ***, $p < 0.001$; n (WT/KO) = 12. *B*, presumably causative for polydipsia, serum osmolality was significantly increased. **, $p < 0.01$; n (WT/KO) = 12. In line with hyperosmolality Na^+ (*C*) and Cl^- (*D*) levels were significantly elevated. ***, $p < 0.001$; n (WT) = 12; n (KO) = 17. All values are mean ± S.D. (*error bars*).

SPRED2 isoform in lysates of WT brain, whereas a prominent 30 kDa band was observed in WT kidney lysates, most likely representing a *Spred2* splice variant. Both proteins were absent in the corresponding KO lysates (Fig. 1*B*, *middle*). Instead, we detected a 150-kDa protein, which was absent in WT lysates and migrated with the calculated molecular mass of the EHV1-β-geo fusion protein (134-kDa β-geo plus 16-kDa N-terminal SPRED2; Fig. 1*B*, *top*). Consistently, anti-β-gal antibodies also detected the 150 kDa band, thereby confirming the expression of the EVH1-β-geo fusion protein in KO mouse organs, and identified additionally a second protein with an apparent molecular mass of about 135 kDa (Fig. 1*B*, *bottom*). Because this band was absent in blots with anti-SPRED2 antibodies, it most likely corresponds to the non-fused β-geo protein, which contains its own internal start codon (Fig. 1*A*). To analyze functionality of the fusion protein, we cloned EVH1-β-geo and β-geo, respectively, and expressed both in HEK293 cells. Expression of proteins was confirmed by Western blotting (Fig. 1*C*), and X-Gal staining of transfected cells verified the enzymatic activity of the fusion construct, thereby reflecting proper expression of the fusion protein (Fig. 1*D*).

Hyperosmolality Induced by Elevated Serum Salt Concentrations Correlates with Polydipsia in SPRED2$^{-/-}$ Mice—SPRED2 KO mice had an obviously greater water demand than their WT littermates. Therefore, drinking behavior of WT and KO animals was examined over a period of 1 month. Calculation of daily water consumption in relation to body weight revealed a nearly doubled water uptake of SPRED2$^{-/-}$ mice (Fig. 2*A*). Enhanced thirst and increased water consumption correlated with a significantly elevated serum osmolality in SPRED2$^{-/-}$ animals (Fig. 2*B*). Hyperosmolality was accompanied by significantly higher serum Na^+ (Fig. 2*C*) and Cl^- (Fig. 2*D*) concentrations. Altogether, our findings demonstrated striking salt and water imbalances in our SPRED2$^{-/-}$ mice.

TABLE 1

Serum parameters and growth hormone levels in WT and SPRED2$^{-/-}$ mice

Results are expressed as mean ± S.D. n (WT/KO) ≥ 10 for all parameters. GGT, γ-glutamyltransferase; GOT/AST, glutamate oxaloacetate transaminase/aspartate aminotransferase; GPT/ALT, glutamate pyruvate transaminase/alanine aminotransferase; CK, creatine kinase; GH, growth hormone, IGF-1, insulin-like growth factor 1.

Parameter	WT	KO
Osmolality (mosmol/kg)	310.3 ± 7.8	318.3 ± 4.6[a]
Na^+ (mmol/liter)	146.3 ± 2.3	152.1 ± 4.2[b]
Cl^- (mmol/liter)	114.4 ± 1.6	120.7 ± 4.1[b]
K^+ (mmol/liter)	5.2 ± 1.1	4.9 ± 0.5
Ca^+ (mmol/liter)	2.2 ± 0.1	2.2 ± 0.2
PO_4^{3-} (mmol/liter)	2.4 ± 0.2	2.4 ± 0.4
Urea (mg/dl)	38.4 ± 11.1	51.9 ± 26.3
Creatinine (mg/dl)	0.12 ± 0.04	0.10 ± 0.00
Uric acid (mg/dl)	0.88 ± 0.47	0.81 ± 0.36
Glucose (mg/dl)	216.6 ± 52.7	140.6 ± 28.3[b]
Triglyceride (mg/dl)	72.8 ± 10.7	51.5 ± 18.3[c]
Cholesterol (mg/dl)	154.4 ± 32.6	109.0 ± 24.1[a]
Alkaline phosphatase (units/liter)	69.4 ± 27.3	48.8 ± 13.3[c]
Cholinesterase (units/liter)	7,985 ± 1,178	6,354 ± 2,239
Albumin (g/dl)	2.9 ± 0.3	2.7 ± 0.3
Bilirubin (mg/dl)	0.10 ± 0.00	0.12 ± 0.04
Iron (µg/dl)	150.8 ± 25.8	146.9 ± 30.7
GGT (units/liter)	0.10 ± 0.00	0.10 ± 0.00
GOT/AST (units/liter)	145.5 ± 71.2	69.2 ± 18.6[c]
GPT/ALT (units/liter)	73.1 ± 35.5	34.4 ± 9.4[c]
Total CK (units/liter)	636.2 ± 242.3	101.2 ± 42.1[a]
Total protein (g/dl)	4.9 ± 0.3	4.9 ± 0.7
Amylase (units/liter)	2,870 ± 522	2,954 ± 757
Lipase (units/liter)	26.7 ± 12.1	18.7 ± 5.2
Lactat dehydrogenase (units/liter)	363.8 ± 120.9	279.7 ± 179.4
GH (ng/ml)	2.9 ± 2.7	8.1 ± 5.2[a]
IGF-1 (ng/ml)	381.6 ± 104.9	604.9 ± 212.1[b]

[a] $p < 0.01$.
[b] $p < 0.001$.
[c] $p < 0.05$.

Further Changes in Parameters Affecting Growth and Body Homeostasis—Because enhanced drinking is often accompanied by kidney dysfunction and changes in blood test results, common serum parameters of WT and KO mice were determined (see Table 1, a survey of analyzed parameters).

Because levels of other osmolytes, like Ca^+, PO_4^{3-}, and K^+, were unchanged or reduced, hyperosmolality most likely originated from higher blood NaCl load (Fig. 2, *C* and *D*). K^+ levels, however, tended to be decreased. Together with the observed hypernatremia, this was an indication for hyperaldosteronism.

Kidney parameters, like urea, creatinine, and uric acid, were not significantly changed. Because of a 35% reduction in serum glucose and nearly 30% in triglycerides and cholesterol, we excluded diabetes mellitus as the reason for polydipsia.

Liver parameters and others, like cholinesterase, albumin, bilirubin, iron, γ-glutamyltransferase (GGT), total protein, amylase, lipase, and lactate dehydrogenase did not differ between WT and SPRED2$^{-/-}$ mice or even tended to be lower in the KOs. Although glutamate oxaloacetate transaminase/aspartate aminotransferase (GOT/AST), glutamate pyruvate transaminase/alanine aminotransferase (GPT/ALT), and total creatine kinase (CK) were dramatically reduced in the KOs, a decrease in these parameters normally has no diagnostic relevance but suggests an impaired energy balance in SPRED2$^{-/-}$ mice.

In line with the dwarf phenotype of SPRED2-deficient mice (28), alkaline phosphatase was 30% decreased, which is indicative for achondroplasia. Surprisingly, despite the described dwarfism in SPRED2 KO mice (28), serum levels of GH were

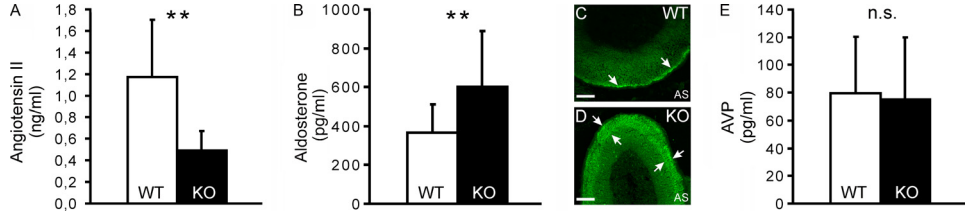

FIGURE 3. **SPRED2-deficiency causes dysregulation of salt and water homeostasis-controlling hormones.** *A*, Ang II, a primary stimulator of aldosterone release, was halved in KO mice. **, $p < 0.01$; *n* (WT) = 10; *n* (KO) = 12. *B*, in line with hyperosmolality and increased blood salt load, but despite reduced Ang II secretion, serum aldosterone was almost doubled in SPRED2-deficient mice. **, $p < 0.01$; *n* (WT/KO) = 14. Immunohistochemistry of AS in adrenal glands of WT (*C*) and SPRED2$^{-/-}$ (*D*) mice exhibited broadened localization of AS in KO tissues, normally restricted to the zona glomerulosa (*arrows*). *Scale bars*, 200 μm. *E*, for AVP, no significant differences could be detected upon water deprivation. *n.s.*, not significant; *n* (WT) = 10; *n* (KO) = 17. All values are mean ± S.D. (*error bars*).

TABLE 2

Body weights, adrenal, kidney, and brain weight/body weight ratios, as well as serum osmolalities of WT and SPRED2$^{-/-}$ mice under basal conditions and after 48 h of water deprivation

Results are expressed as mean ± S.D. Significance is displayed as follows. A, WT non-deprived *versus* KO non-deprived; B, WT deprived *versus* KO deprived; C, WT non-deprived *versus* WT deprived; *D*, KO non-deprived *versus* KO deprived. For all parameters, *n* (WT/KO) ≥ 10. BW, body weight.

Parameter	Control group		Water deprivation (48 h)		Significance
	WT	KO	WT	KO	
BW (g)	36.6 ± 7.1	23.9 ± 4.0	32.2 ± 7.0	19.3 ± 3.7	A[a]; B[a]; D[b]
BW reduction (%)			12.02	19.25	
Adrenal gland weight/BW ratio (%)	0.014 ± 0.005	0.019 ± 0.006	0.018 ± 0.007	0.028 ± 0.007	A[c]; B[b]; D[a]
Adrenal gland weight/BW ratio increase (%)			28.57	47.37	
Kidney weight/BW ratio (%)	1.1 ± 0.2	1.3 ± 0.1	1.2 ± 0.3	1.7 ± 0.2	A[b]; B[a]; D[a]
Kidney weight/BW ratio increase (%)			9.09	30.77	
Brain weight/BW ratio (%)	1.6 ± 0.4	2.1 ± 0.2	1.7 ± 0.3	2.7 ± 0.5	A[b]; B[c]; D[a]
Brain weight/BW ratio increase (%)			6.25	28.57	
Serum osmolality (mosmol/kg)	310.3 ± 7.8	318.3 ± 4.6	331.8 ± 6.2	357.6 ± 23.3	A[b]; B[a]; C[a]; D[a]
Serum osmolality increase (%)			6.93	12.35	

[a] $p < 0.001$.
[b] $p < 0.01$.
[c] $p < 0.05$.

nearly 3-fold elevated, and serum levels of IGF-1 were increased by 60% as compared with littermate controls.

Enhanced Aldosterone Release and Increase in Aldosterone Synthase Provoke Salt and Water Imbalances in SPRED2 KO Mice—Aldosterone is one potent regulator of fluid and salt homeostasis, and its release is mainly regulated by K^+ and activation of the RAS. To clarify whether hyperosmolality and increased serum salt load in SPRED2$^{-/-}$ mice were due to an up-regulation of the RAS, we estimated aldosterone and Ang II in serum of WT and KO mice by enzyme immunoassay. Whereas the Ang II concentration in KO mice was reduced by over 50% as compared with WT controls (Fig. 3*A*), aldosterone was almost doubled in SPRED2$^{-/-}$ mice (Fig. 3*B*). Therefore, in SPRED2 KO mice, the RAS seemed to be down-regulated, and K^+ levels were not increased, thus suggesting the involvement of another trigger causing hyperaldosteronism.

The elevated serum aldosterone concentrations of SPRED2 KO mice pointed to an up-regulated release by aldosterone-producing cells in the zona glomerulosa of the adrenal cortex. In WT adrenal glands, AS staining showed restricted expression in the zona glomerulosa, a thin layer at the border of the adrenal cortex (Fig. 3*C*). In contrast, adrenocortical zonation was destroyed in SPRED2$^{-/-}$ mice, either because the regular AS expansion was broadened to the zona fasciculata, located in the middle part of adrenal cortex, or the zona glomerulosa itself was expanded (Fig. 3*D*). Thus, the number of AS-producing cells seemed to be substantially increased and causative for enhanced aldosterone secretion.

Augmented Loss of Body Fluid but Unaffected AVP Secretion after Water Deprivation in SPRED2-deficient Mice—AVP stimulates water retention in the kidney upon serum hyperosmolality. Based on the increased blood salt load associated with polydipsia in SPRED2 KO mice, we wondered if an AVP release disorder was involved in the fluid and salt imbalances. To analyze water retention and AVP release, we investigated organ/body weight ratios of adrenals, kidneys, and brains, as well as serum osmolalities, and AVP levels by enzyme immunoassay before and after 48 h of water deprivation in WT and SPRED2$^{-/-}$ mice (Table 2). Because loss of SPRED2 causes hypochondroplasia-like dwarfism (28), which is associated with a reduced body weight in the KOs already before water deprivation, we focused on the relative body weight and organ weight changes. Water starvation significantly reduced the body weight within the KO group. Accordingly, the relative percentage body weight reduction was about 12% in WT but notably higher, ~19%, in SPRED2-deficient mice. Comparing SPRED2-deficient mice before and after water deprivation, a dramatic increase of organ/body weight ratios was detected for brains, adrenal glands, and kidneys, but no significant changes could be seen within the WT group. In WT mice, water deprivation led to an increase in organ/body weight ratios, with nearly 29% in adrenals, 9% in kidneys, and 6% in brains. However, in SPRED2$^{-/-}$ mice, the increase of all organ/body weight ratios was significant, and with at least 20% substantially stronger, rising up to 47% in adrenals, to 31% in kidneys, and to 29% in brains. As demonstrated previously (see Fig. 2*B* and Table 1),

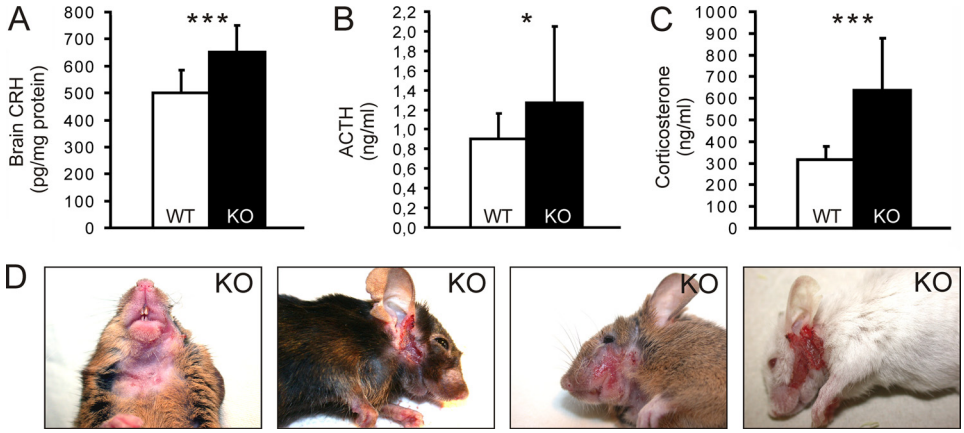

FIGURE 4. **Up-regulation of HPA hormone secretion is accompanied by obsessive overgrooming in SPRED2$^{-/-}$ mice.** Stress hormones secreted successively by organs of the HPA axis were significantly elevated in SPRED2-deficient mice, demonstrated by a 30% increase of CRH in PVN region-containing brain lysates (***, $p < 0.001$; n (WT/KO) = 20 (*A*); a 30% increase of serum ACTH (*, $p < 0.05$; n (WT) = 17; n (KO) = 22) (*B*); and a more than doubled serum corticosterone level (***, $p < 0.001$; n (WT/KO) = 12) (*C*). *D*, SPRED2$^{-/-}$ mice developed self-inflicted severe skin lesions on their face, neck, and snout originating from compulsive grooming behavior. All values are mean ± S.D. (*error bars*).

serum osmolality of SPRED2-deficient mice was significantly elevated over WT controls even under basal conditions. Although the increase of serum osmolality after water deprivation was significant within both genotypes, the elevation was almost doubled in SPRED2 KO mice shown by a 12% increase, in contrast to an only 7% increase in WT animals. In summary, the water deprivation experiment clearly shows that water retention is impaired in SPRED2-deficient mice, leading to a stronger decreased body weight, a more elevated organ/body weight ratio, and a further increased serum osmolality after dehydration. Because AVP stimulates water retention in the kidney, we investigated whether reduced AVP secretion could explain the decreased water retention. Remarkably, we could not detect any differences between WT and KO AVP levels after water deprivation (Fig. 3*E*), leading us to the assumption that a dysregulation of AVP secretion might not be the reason for polydipsia in SPRED2-deficient mice.

Overshooting HPA Hormone Secretion in SPRED2$^{-/-}$ Mice Is Associated with Excessive Self-grooming—In addition to K^+ and the RAS, ACTH is another effective regulator of aldosterone release, and, together with CRH and corticosterone, also a potent mediator of stress responses. CRH, secreted by the hypothalamus and, therefore, the most upstream acting hormone of the HPA axis, was significantly increased by about 30% in paraventricular nucleus (PVN)-containing brain lysates of KO animals (Fig. 4*A*). Accordingly, serum levels of ACTH, positively regulated by CRH and released downstream by the pituitary gland, were also 30% elevated (Fig. 4*B*), and corticosterone (Fig. 4*C*), which is produced upon ACTH stimulation by the adrenal gland, was more than doubled in SPRED2-deficient mice. Taken together, stress hormone release was up-regulated at all levels of the HPA axis.

Augmented HPA hormone secretion is often the consequence of stress-associated pathologies and mood swings. SPRED2 KO mice older than 4 months developed severe skin lesions, usually first noticed as small wounds at the snout or cheek and progressing to uni- or bilateral lesions encompassing large parts of the neck or face (Fig. 4*D*). These lesions occurred in SPRED2-deficient mice regardless of whether they were housed alone or together with cage mates and were not observed in WT mice, even when kept in one cage with KO mice. SPRED2 KO mice were not found to behave aggressively or busy in grooming other cage mates but were often seen engaged in self-grooming both when housed alone or in groups. Closer observations of this behavior demonstrated that SPRED2-deficient mice spent obviously more time for grooming than their WT littermates and showed excessive and injurious levels of self-grooming bouts, regardless of the time of day. This phenotype is reminiscent of compulsive disorders and very likely associated with up-regulation of the HPA system.

SPRED2 Expression and Spred2 Promoter Activity in Phenotype-related Tissues—SPRED2 is almost ubiquitously expressed in mouse tissues, as previously demonstrated on RNA and protein levels and by *Spred2* promoter activity studies (26, 27). In order to prove the expression in organs involved in the phenotypical pathologies, we especially examined tissues of the HPA axis. Therefore, we visualized the expression pattern of SPRED2 by immunohistochemistry of WT tissue sections and *Spred2* promoter activity by X-Gal staining of heterozygous (HET) organs and sections. In the hypothalamus, where CRH and AVP are produced, both *Spred2* promoter activity and SPRED2 expression were evenly distributed in the entire organ (Fig. 5, *A–C*). In the pituitary gland, which releases ACTH in the anterior and AVP in the posterior part, SPRED2 protein was also present in the whole organ but enriched in the posterior tract (Fig. 5, *D–F*). Adrenal glands, secreting aldosterone from the zona glomerulosa and corticosterone from the zona fasciculata, were positive for SPRED2 expression and promoter activity, predominantly in a thin layer at the border of the adrenal cortex tracking the zona glomerulosa (Fig. 5, *G–I*).

SPRED Is a Negative Regulator of CRH Production in Vitro and in Vivo—Because SPREDs have been shown to be negative regulators of MAPK signaling (23), we examined ERK expression and phosphorylation in the same brain lysates used for CRH ELISA. Western blot analysis in both 6- and 12-month-old animals revealed a significantly increased ERK phosphorylation in the KOs (Fig. 6*A*). Due to the loss of SPRED-mediated inhibition, we detected an over 2.5-fold elevated ratio of phos-

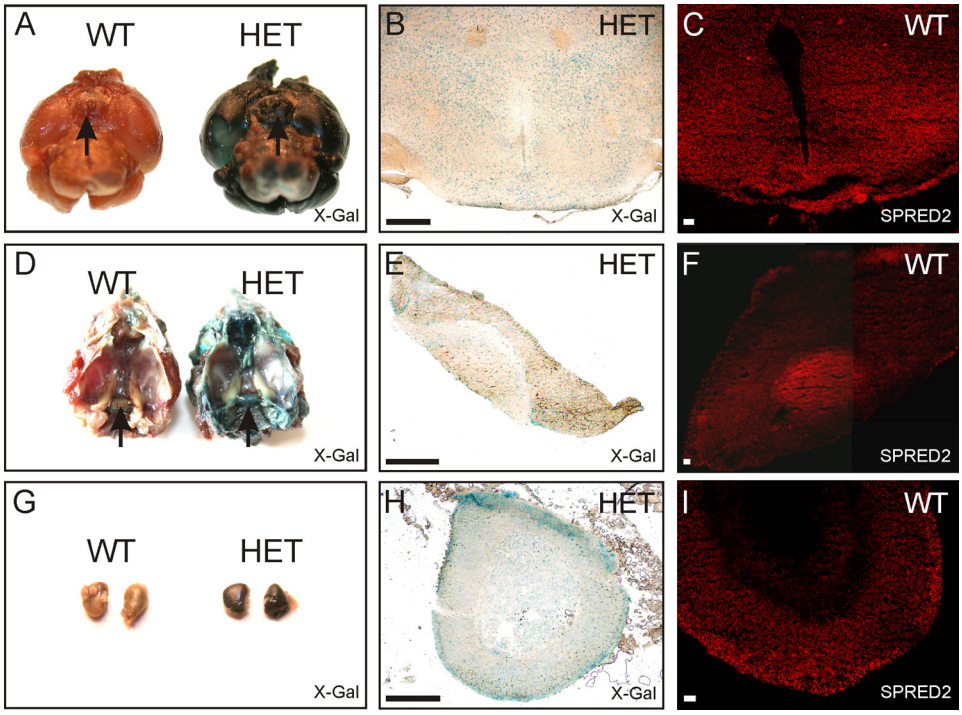

FIGURE 5. ***Spred2* expression profiling in organs of the HPA axis.** X-Gal stainings of whole WT and HET organs (*arrows*) (*A*, *D*, and *G*) and tissue sections of SPRED2$^{+/-}$ mice (*B*, *E*, and *H*) demonstrated endogenous *Spred2* promoter activity. *C*, *F*, and *I*, on protein level, SPRED2 expression was confirmed by immunohistochemistry with tissue sections of WT mice. Uniform expression was observed in hypothalamus (*A*, *B*, and *C*) and pituitary gland (*D*, *E*, and *F*). *G–I*, in adrenal gland, SPRED2 was predominantly expressed in zona glomerulosa. *Scale bars*, 500 μm (*B*, *E*, and *H*) and 50 μm (*C*, *F*, and *I*).

phorylated ERK to ERK in both age groups of SPRED2$^{-/-}$ mice (Fig. 6*B*). In order to investigate downstream signaling of phospho-ERK and its effect on CRH transcription, we cloned a luciferase reporter vector containing the 5.7-kb region of the 5′ CRH promoter sequence, including exon 1. The CRH promoter comprises a manifold set of transcription factor-binding sites, among others six Ets-binding sites (Fig. 6*C*, *top*). mHypoE-44 cells were transiently transfected with the CRH promoter firefly luciferase reporter, a *Renilla* luciferase control reporter, and with SPRED1 or SPRED2, respectively, either in the presence or absence of EVH1-β-geo. These assays revealed a SPRED-dependent suppression of relative luciferase activity and therefore a down-regulation of CRH promoter activity to 60%. Co-transfection of EVH1-β-geo did not have a further effect on CRH transcription (Fig. 6*C*, *bottom*). To confirm that Ets-binding sites in the CRH promoter are critical for CRH transcription, we performed luciferase reporter assays with a 4xEts reporter using the same experimental setup (Fig. 6*D*, *top*) Thereby, we detected a 90% reduction of Ets-dependent transcription by SPREDs, which was not further influenced by EVH1-β-geo co-expression (Fig. 6 *D*, *bottom*). In line with that, CRH secretion was reduced to 70% by SPRED1 and to 60% by SPRED2, as we could show by CRH ELISA with cell culture supernatants of transfected mHypoE-44 cells (Fig. 6*E*). To investigate if SPREDs play a role in the regulation of ERK-dependent transcription and of CRH promoter activity not only *in vitro* but also *in vivo*, we analyzed the CRH mRNA contents of mouse hypothalamic PVN regions. In quantified Northern blots, we found a 60% increase of CRH mRNA in the KO mice (Fig. 6*F*), which was accompanied by an elevated hypothalamic CRH release (Fig. 4*A*), both together causative for the up-regulated HPA hormone production.

DISCUSSION

Disruption of SPRED2 in mice allowed the characterization of physiological functions of this MAPK inhibitor and the identification of SPRED2 as a novel regulator of HPA axis and body homeostasis. Our mouse model combines the functional KO of SPRED2 with the possibility of gene expression profiling by X-Gal staining (27, 28, 40). Here, we could show that the gene trap resulted in a loss of full-length SPRED2 and of possible organ-specific splice variants, as for example detected in kidney and in liver (22) (GenBank^{TM} accession numbers NM_181784 and NM_001128210). Besides the sole β-geo reporter, we detected the expression of a fusion protein comprising the EVH1 domain and the β-geo reporter under control of the endogenous *Spred2* promoter, resulting from the gene trap vector insertion in intron 4. The functionality of both proteins was confirmed by X-Gal staining, even so, this is accompanied by a complete loss of functional SPRED2 protein in our KO mice.

One of the most obvious observations resulting from the SPRED2 deletion in mice was polydipsia, characterized by nearly doubled daily water consumption. Polydipsia is mainly caused by an impaired renal urine-concentrating ability, and the most frequent reasons for that are diabetes mellitus, diabetes insipidus, and osmotic disorders. Due to clearly reduced serum glucose, triglyceride, and cholesterol levels, we could exclude diabetes mellitus. For diabetes insipidus, the most prevalent cause is lack or insufficient production of AVP. Despite dramatic changes in body weight, organ/body weight

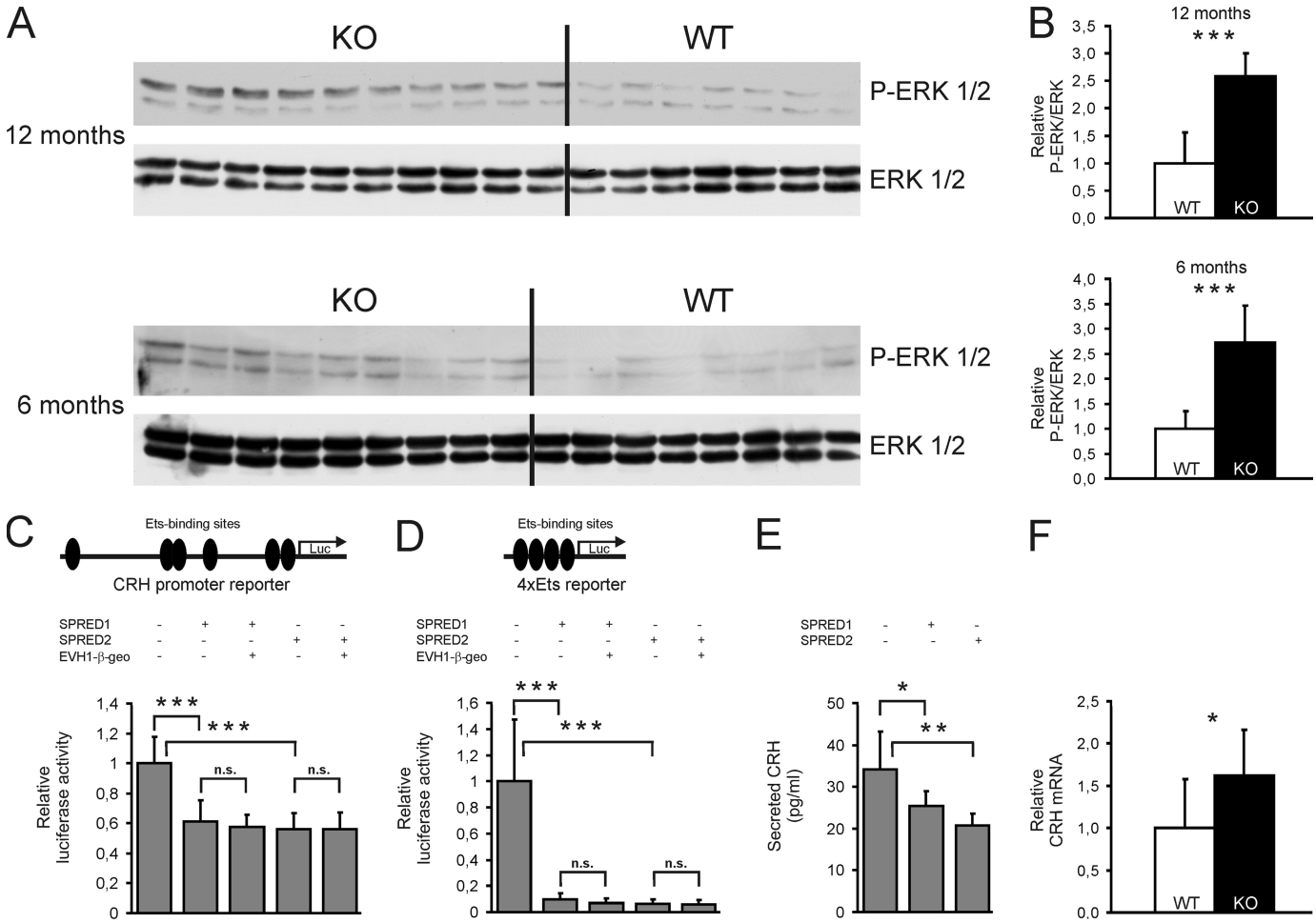

FIGURE 6. ***In vivo* and *in vitro* suppression of CRH production by SPRED.** *A*, Western blot analysis with anti-ERK and anti-phospho-ERK (*P-ERK*) antibodies revealed an increased MAPK signaling in PVN-containing brain regions of both 6- and 12-month-old SPRED2$^{-/-}$ mice. *B*, quantification of ERK and phospho-ERK signals demonstrated a more than 2.5-fold increase of the phospho-ERK/ERK ratio in young and aged SPRED2 KO mice. ***, $p < 0.001$; n (WT) ≥ 7; n (KO) ≥ 8. *C*, *top*, schematic depiction of the cloned CRH promoter reporter with the approximate position of predicted Ets-binding sites. *C*, *bottom*, luciferase reporter assays revealed a 40% reduction of the relative CRH promoter activity by SPRED1 and SPRED2, respectively. No further effect was detected by EVH1-β-geo co-expression. ***, $p < 0.001$; *n.s.*, not significant; $n = 12$. *D*, *top*, schematic depiction of the 4xEts reporter. *D*, *bottom*, suppression of luciferase reporter activity to ~10% by SPRED1 and SPRED2, respectively. EVH1-β-geo co-expression showed no further effect. ***, $p < 0.001$; *n.s.*, not significant; $n = 12$. *E*, CRH production in mHypoE-44 cells was reduced to 70% by SPRED1 and to 60% by SPRED2, as determined in cell culture supernatants by ELISA. *, $p < 0.05$ for SPRED1; **, $p < 0.01$ for SPRED2; $n = 12$. *F*, Northern blot analysis with RNA from the PVN-containing hypothalamus of SPRED2 KO mice demonstrated a 60% increase of CRH mRNA. *, $p < 0.05$; n (WT) $= 9$; n (KO) $= 8$. All values are mean ± S.D. (*error bars*).

ratios, and serum osmolalities, no differences in AVP release after water deprivation were detected in our experimental setup, which excludes diabetes insipidus-induced polydipsia and suggests a negligible role for SPRED-mediated MAPK signaling in regulation of AVP secretion. Nevertheless, compared with the already substantial loss of body weight in WT mice, the body weights of KO mice were even further reduced after water deprivation, which demonstrated an extreme loss of body fluid. Accordingly, adrenal, kidney, and brain weight/body weight ratios were increased, a phenomenon that has already been shown for adrenals and kidneys in similar experiments (41, 42). However, the observed fluid loss and polydipsia pointed to an impaired water reabsorbtion or to an osmotic imbalance.

Indeed, enhanced drinking was accompanied by elevated Na^+ and Cl^- serum levels, leading to serum hyperosmolality in SPRED2$^{-/-}$ mice. Similar phenotypes have been described for KO mouse models of AQP2 (43, 44), the AVP receptor 2 (45), the renal Na^+-K^+-$2Cl^-$ cotransporter (46), and the renal outer medullary potassium channel (47), all implicating defects in the renal urine-concentrating mechanisms and all developing hydronephrosis. Serum electrolyte concentrations in these models were either unaffected (43, 44) or regarded as secondary effects of dehydration and fluid loss (45–47). In our SPRED2$^{-/-}$ mice, elevated Na^+ and Cl^- serum levels and the resulting hyperosmolality were additionally supported by hyperaldosteronism, characterized by nearly doubled aldosterone levels in SPRED2$^{-/-}$ mice. From these data, we conclude that our SPRED2$^{-/-}$ mice might display a combination of both an increased sodium retention that cannot be compensated for by the higher water uptake and a urinary concentrating defect.

Despite hyperaldosteronism, the aldosterone release-stimulating serum K^+ was rather reduced in KO animals and thus seemed not to be the reason for the elevated serum aldosterone. Similarly, the RAS also could be excluded as the cause of hyperaldosteronism because Ang II was decreased by over 50% in the KO mice. The low serum Ang II could be due to the feedback

inhibition of renin release by aldosterone and indicates the presence of another effective stimulus of aldosterone secretion in our SPRED2 KO mice.

A common disease characterized by symptoms like hypernatremia, hypokalemia, and increased aldosterone in connection with a lower RAS activity is primary hyperaldosteronism (Conn syndrome), caused by an autonomous aldosterone overproduction in the adrenal zona glomerulosa. Conn syndrome constitutes more than 10% of hypertension worldwide, but unexpectedly, SPRED2$^{-/-}$ mice were normotensive (data not shown). Previous studies demonstrated, however, that not all mouse strains are susceptible to aldosterone-induced hypertension (48, 49).

During aldosterone biosynthesis, taking place in the adrenal zona glomerulosa, the last three steps from 11-deoxycorticosterone to aldosterone are mediated by aldosterone synthase (12, 13). AS staining revealed an obviously broadened expression in the adrenal cortex of SPRED2$^{-/-}$ mice, a phenotype similar to that observed in female TASK1$^{-/-}$ mice, thereby resembling the SPRED2 KO mice in the increase and expansion of aldosterone-producing cells, hyperaldosteronism, and diminished RAS activity (50). In our SPRED2$^{-/-}$ mouse model, the elevated adrenal weight/body weight ratios and the functional corticosterone production in the zona fasciculata, attested by elevated corticosterone levels, pointed toward a hyperplasia of aldosterone-producing cells in the zona glomerulosa rather than to a mislocalization of them into the zona fasciculata. This assumption was further supported by adrenal SPRED2 expression predominantly in the zona glomerulosa. The hyperplasia of aldosterone-producing cells might be caused by an up-regulated MAPK pathway due to the loss of SPRED2-mediated inhibition. Consistently, increased ERK phosphorylation has been shown to induce proliferation in adrenals, as reviewed in Ref. 51, and specifically in zona glomerulosa cells (52) in response to ACTH. This increase in the number of AS-expressing cells might then account for hyperaldosteronism and, similar to TASK1, SPRED2-regulated MAPK signaling might be unraveled as another mechanism required for the regular adrenocortical zonation and appropriate AS expression in the zona glomerulosa.

Besides augmented AS expression, ACTH was also increased by 30% in SPRED2-deficient mice. ACTH exerts both trophic (51, 52) and steroidogenic effects on the adrenal gland. The acute response to ACTH stimuli leads to the mobilization of cholesterol and the subsequent generation of corticosterone in the adrenal zona fasciculata and of aldosterone in the zona glomerulosa cells (5). The chronic ACTH effect directs transcription of genes encoding the enzymes required for steroidogenesis (53, 54). Especially 11β-hydroxylase, the critical enzyme in corticosterone synthesis, is regulated by ACTH (55), whereas AS expression seems to be mainly controlled by the RAS and K^+ (56). Therefore, first, the hypercorticosteronism in SPRED 2$^{-/-}$ mice is probably due to increased serum ACTH. Second, because in mice, biosynthesis pathways of aldosterone and corticosterone are homologous up to corticosterone, a combination of both the elevated ACTH leading to an increase in the aldosterone precursor corticosterone and the hyperplasia of AS-expressing adrenal zona glomerulosa cells might contribute to the hyperaldosteronism in SPRED2 KO mice.

To clarify ACTH overproduction, we determined CRH in brain lysates and detected a significant elevation of about 30% in KO mice. Therefore, we believed that an up-regulation of the entire HPA axis was responsible for increased levels of downstream hormones. Various transgenic mouse lines overexpressing CRH also exhibited elevated ACTH and corticosterone secretion associated with adrenal hypertrophy and Cushing disease (57, 58). Furthermore, these mouse models are susceptible to stress-associated diseases (59–61). In contrast, genomic ablation of CRH receptor 1 exhibited an impaired stress response and impaired anxiety behavior (62). Up-regulation of hormone secretion along the HPA axis, one major mediator of stress responses, has also been shown to be involved in affective disorders in humans (7, 8). Mice lacking SAP90/PSD95-associated protein 3, a postsynaptic scaffolding protein highly expressed at excitatory striatal synapses, develop severe facial lesions due to an obsessive-compulsive grooming disorder (63). In agreement, SPRED2 KO mice also show compulsive grooming leading to self-inflicted lesions. This reflects apparent signs of chronic stress in SPRED2 KO mice, in this case most likely caused by HPA hormone overproduction.

SPRED1 has been shown to be expressed predominantly in the brain (21, 26) and to be enriched in the central nervous system, where it mediates cortical development, neural stem cell proliferation, and vesicular trafficking (26, 37). Recently, it has been shown that germ line loss-of-function mutations of SPRED1 cause the neurofibromatosis type 1-like Legius syndrome, associated with café-au-lait spots, facial abnormalities, and behavioral and learning problems (31, 33–35). Reduced body weight, shortened face, and impaired hippocampus-dependent learning in SPRED1$^{-/-}$ mice (29, 31, 36) resemble the SPRED1-deficient phenotype in humans and may relate to dwarfism and facial abnormalities seen in SPRED2 KO mice (28). Despite this dwarf phenotype, levels of GH and IGF-1 were surprisingly found to be elevated. Analogous to ACTH, GH is secreted by the anterior pituitary and stimulates the production of its downstream effector IGF-1. Therefore, overproduction of growth hormones might be a further consequence of the generalized up-regulation of the HPA axis in SPRED2 KO mice. Obviously, the increased GH and IGF-1 levels are not sufficient to feed back to HPA organs and not sufficient to overcome the hypochondroplasia-like dwarf phenotype. A well known elicitor of dwarfism apart from growth factor deficiencies and disorders is the missing inhibition of MAPK signaling downstream of the fibroblast growth factor receptor 3 (64). This endochondral ossification defect has also been shown to be causative for dwarfism in our SPRED2 KO mice (28).

In addition to the expression of SPRED2 in the brain (26, 27), we could demonstrate SPRED2 expression and promoter activity in the hypothalamus, pituitary, and adrenals. The release of HPA stress hormones from these glands is triggered by the limbic system. It comprises a set of brain structures, including the limbic cortex, hippocampus, amygdala, and also the hypothalamus, which activates the HPA axis by CRH secretion. In hypothalami of SPRED2$^{-/-}$ mice, we detected a significantly increased ERK phosphorylation, demonstrating an up-regu-

lated MAPK signaling. There is emerging evidence that SPRED2 is not only present in tissues of the HPA axis but also that MAPK pathways for which SPREDs serve as inhibitors are involved in the regulation of the HPA axis. In this manner, various stimuli (*e.g.* chronic stress, prolactin, hypoglycemia, and lipopolysaccharides) cause an activation of the MAPK signaling pathway and phosphorylation of downstream transcription factors in the hypothalamus (15–17) and also in the limbic system (18). The increase in ERK phosphorylation in the CRH-producing neurons, located in the hypothalamic PVN, always involves a parallel activation of CRH transcription in these neurons (15–17). In mHypoE-44 cells, CRH promoter activity was suppressed by SPRED. The CRH promoter comprises a variety of transcription factor binding sites, of which six were predicted to represent MAPK-regulated Ets-binding sites (19). Indeed, SPRED1 and -2 were also able to suppress an Ets-dependent reporter.

In both reporter assays, we could not detect an influence of the EVH1-β-geo fusion protein on transcriptional regulation. There is evidence that EVH1 domains of SPREDs act dominant negative (25), but for an efficient suppression of MAPK signaling, both the EVH1 and the SPR domains seem to be required (24). This led us to the assumption that the aberrant expression of EVH1-β-geo does not affect the MAPK-dependent regulation of the HPA axis.

Besides CRH transcription, CRH secretion was also inhibited by SPREDs in mHypoE-44 cells. In line with these *in vitro* data, we detected higher CRH mRNA contents in hypothalami of KO mice, paralleled by an increased CRH secretion. Because the suppressive effect of SPRED2 is restricted to the MAPK pathway (23–25), it seems reasonable that the up-regulated MAPK signaling in our KO mice probably leads to an augmented ERK/Ets-dependent CRH transcription and release, resulting in an overproduction of hormones at all levels of the HPA axis.

In summary, we demonstrated that SPRED2-mediated inhibition of the MAPK/ERK/Ets signaling pathway is essential for appropriate regulation of the HPA axis and body homeostasis. Our SPRED2$^{-/-}$ mice show an up-regulated MAPK signaling in the brain and increased hypothalamic CRH mRNA levels and release, most likely causing obsessive grooming and elevated hormone secretion at all levels of the HPA axis. Hyperaldosteronism, probably resulting from HPA up-regulation in combination with the increase in aldosterone synthase, leads to salt and water imbalances and comorbidities. Further investigations will show how this overactivated HPA axis influences behavior and stress response and if a human correlate exists.

Acknowledgments—We are thankful to Celso E. Gomez-Sanchez (Division of Endocrinology, GV Montgomery Veterans Affairs Medical Center, Jackson, MS) for providing aldosterone synthase-specific antibodies and technical support and the Central Laboratory of the University Clinic (Wuerzburg, Germany) for estimating serum parameters.

REFERENCES

1. Vale, W., Spiess, J., Rivier, C., and Rivier, J. (1981) *Science* **213,** 1394–1397
2. Rivier, C., Brownstein, M., Spiess, J., Rivier, J., and Vale, W. (1982) *Endocrinology* **110,** 272–278
3. Smith, A. I., and Funder, J. W. (1988) *Endocr. Rev.* **9,** 159–179
4. Papadimitriou, A., and Priftis, K. N. (2009) *Neuroimmunomodulation* **16,** 265–271
5. James, V. H. (1992) *The Adrenal Gland*, 2nd Ed., pp. 71–87, Raven Press, New York
6. Seasholtz, A. (2000) *J. Clin. Invest.* **105,** 1187–1188
7. Bao, A. M., Meynen, G., and Swaab, D. F. (2008) *Brain Res. Rev.* **57,** 531–553
8. Pariante, C. M., and Lightman, S. L. (2008) *Trends Neurosci.* **31,** 464–468
9. Dunn, F. L., Brennan, T. J., Nelson, A. E., and Robertson, G. L. (1973) *J. Clin. Invest.* **52,** 3212–3219
10. Nielsen, S., Marples, D., Frøkiaer, J., Knepper, M., and Agre, P. (1996) *Kidney Int.* **49,** 1718–1723
11. Spät, A., and Hunyady, L. (2004) *Physiol. Rev.* **84,** 489–539
12. Giroud, C. J., Stachenko, J., and Venning, E. H. (1956) *Proc. Soc. Exp. Biol. Med.* **92,** 154–158
13. Curnow, K. M., Tusie-Luna, M. T., Pascoe, L., Natarajan, R., Gu, J. L., Nadler, J. L., and White, P. C. (1991) *Mol. Endocrinol.* **5,** 1513–1522
14. Rossi, G. P., Sechi, L. A., Giacchetti, G., Ronconi, V., Strazzullo, P., and Funder, J. W. (2008) *Trends Endocrinol. Metab.* **19,** 88–90
15. Khan, A. M., and Watts, A. G. (2004) *Endocrinology* **145,** 351–359
16. Blume, A., Torner, L., Liu, Y., Subburaju, S., Aguilera, G., and Neumann, I. D. (2009) *Endocrinology* **150,** 1841–1849
17. Singru, P. S., Sánchez, E., Acharya, R., Fekete, C., and Lechan, R. M. (2008) *Endocrinology* **149,** 2283–2292
18. Gerrits, M., Westenbroek, C., Koch, T., Grootkarzijn, A., and ter Horst, G. J. (2006) *Neuroscience* **142,** 1293–1302
19. Wasylyk, B., Hagman, J., and Gutierrez-Hartmann, A. (1998) *Trends Biochem. Sci.* **23,** 213–216
20. Seger, R., and Krebs, E. G. (1995) *FASEB J.* **9,** 726–735
21. Kato, R., Nonami, A., Taketomi, T., Wakioka, T., Kuroiwa, A., Matsuda, Y., and Yoshimura, A. (2003) *Biochem. Biophys. Res. Commun.* **302,** 767–772
22. King, J. A., Corcoran, N. M., D'Abaco, G. M., Straffon, A. F., Smith, C. T., Poon, C. L., Buchert, M. I. S., Hall, N. E., Lock, P., and Hovens, C. M. (2006) *J. Hepatol.* **44,** 758–767
23. Wakioka, T., Sasaki, A., Kato, R., Shouda, T., Matsumoto, A., Miyoshi, K., Tsuneoka, M., Komiya, S., Baron, R., and Yoshimura, A. (2001) *Nature* **412,** 647–651
24. King, J. A., Straffon, A. F., D'Abaco, G. M., Poon, C. L., I. S. T., Smith, C. M., Buchert, M., Corcoran, N. M., Hall, N. E., Callus, B. A., Sarcevic, B., Martin, D., Lock, P., and Hovens, C. M. (2005) *Biochem. J.* **388,** 445–454
25. Nonami, A., Kato, R., Taniguchi, K., Yoshiga, D., Taketomi, T., Fukuyama, S., Harada, M., Sasaki, A., and Yoshimura, A. (2004) *J. Biol. Chem.* **279,** 52543–52551
26. Engelhardt, C. M., Bundschu, K., Messerschmitt, M., Renné, T., Walter, U., Reinhard, M., and Schuh, K. (2004) *Histochem. Cell Biol.* **122,** 527–538
27. Bundschu, K., Gattenlöhner, S., Knobeloch, K. P., Walter, U., and Schuh, K. (2006) *Gene Expr. Patterns* **6,** 247–255
28. Bundschu, K., Knobeloch, K. P., Ullrich, M., Schinke, T., Amling, M., Engelhardt, C. M., Renné, T., Walter, U., and Schuh, K. (2005) *J. Biol. Chem.* **280,** 28572–28580
29. Inoue, H., Kato, R., Fukuyama, S., Nonami, A., Taniguchi, K., Matsumoto, K., Nakano, T., Tsuda, M., Matsumura, M., Kubo, M., Ishikawa, F., Moon, B. G., Takatsu, K., Nakanishi, Y., and Yoshimura, A. (2005) *J. Exp. Med.* **201,** 73–82
30. Nobuhisa, I., Kato, R., Inoue, H., Takizawa, M., Okita, K., Yoshimura, A., and Taga, T. (2004) *J. Exp. Med.* **199,** 737–742
31. Brems, H., Chmara, M., Sahbatou, M., Denayer, E., Taniguchi, K., Kato, R., Somers, R., Messiaen, L., De Schepper, S., Fryns, J. P., Cools, J., Marynen, P., Thomas, G., Yoshimura, A., and Legius, E. (2007) *Nat. Genet.* **39,** 1120–1126
32. Taniguchi, K., Kohno, R., Ayada, T., Kato, R., Ichiyama, K., Morisada, T., Oike, Y., Yonemitsu, Y., Maehara, Y., and Yoshimura, A. (2007) *Mol. Cell Biol.* **27,** 4541–4550
33. Messiaen, L., Yao, S., Brems, H., Callens, T., Sathienkijkanchai, A., Denayer, E., Spencer, E., Arn, P., Babovic-Vuksanovic, D., Bay, C., Bobele, G., Cohen, B. H., Escobar, L., Eunpu, D., Grebe, T., Greenstein, R., Hachen, R.,

Irons, M., Kronn, D., Lemire, E., Leppig, K., Lim, C., McDonald, M., Narayanan, V., Pearn, A., Pedersen, R., Powell, B., Shapiro, L. R., Skidmore, D., Tegay, D., Thiese, H., Zackai, E. H., Vijzelaar, R., Taniguchi, K., Ayada, T., Okamoto, F., Yoshimura, A., Parret, A., Korf, B., and Legius, E. (2009) *JAMA* **302,** 2111–2118
34. Pasmant, E., Sabbagh, A., Hanna, N., Masliah-Planchon, J., Jolly, E., Goussard, P., Ballerini, P., Cartault, F., Barbarot, S., Landman-Parker, J., Soufir, N., Parfait, B., Vidaud, M., Wolkenstein, P., Vidaud, D., and France, R. N. (2009) *J. Med. Genet.* **46,** 425–430
35. Spurlock, G., Bennett, E., Chuzhanova, N., Thomas, N., Jim, H. P., Side, L., Davies, S., Haan, E., Kerr, B., Huson, S. M., and Upadhyaya, M. (2009) *J. Med. Genet.* **46,** 431–437
36. Denayer, E., Ahmed, T., Brems, H., Van Woerden, G., Borgesius, N. Z., Callaerts-Vegh, Z., Yoshimura, A., Hartmann, D., Elgersma, Y., D'Hooge, R., Legius, E., and Balschun, D. (2008) *J. Neurosci.* **28,** 14443–14449
37. Phoenix, T. N., and Temple, S. (2010) *Genes Dev.* **24,** 45–56
38. Hoffmeyer, A., Avots, A., Flory, E., Weber, C. K., Serfling, E., and Rapp, U. R. (1998) *J. Biol. Chem.* **273,** 10112–10119
39. Wotus, C., Levay-Young, B. K., Rogers, L. M., Gomez-Sanchez, C. E., and Engeland, W. C. (1998) *Endocrinology* **139,** 4397–4403
40. Ullrich, M., and Schuh, K. (2009) *Methods Mol. Biol.* **561,** 145–159
41. Sebaai, N., Lesage, J., Alaoui, A., Dupouy, J. P., and Deloof, S. (2002) *Eur. J. Endocrinol.* **147,** 835–848
42. Ulrich-Lai, Y. M., Figueiredo, H. F., Ostrander, M. M., Choi, D. C., Engeland, W. C., and Herman, J. P. (2006) *Am. J. Physiol. Endocrinol. Metab.* **291,** E965–E973
43. Rojek, A., Füchtbauer, E. M., Kwon, T. H., Frøkiaer, J., and Nielsen, S. (2006) *Proc. Natl. Acad. Sci. U.S.A.* **103,** 6037–6042
44. Yang, B., Zhao, D., Qian, L., and Verkman, A. S. (2006) *Am. J. Physiol. Renal Physiol.* **291,** F465–F472
45. Yun, J., Schöneberg, T., Liu, J., Schulz, A., Ecelbarger, C. A., Promeneur, D., Nielsen, S., Sheng, H., Grinberg, A., Deng, C., and Wess, J. (2000) *J. Clin. Invest.* **106,** 1361–1371
46. Takahashi, N., Chernavvsky, D. R., Gomez, R. A., Igarashi, P., Gitelman, H. J., and Smithies, O. (2000) *Proc. Natl. Acad. Sci. U.S.A.* **97,** 5434–5439
47. Lorenz, J. N., Baird, N. R., Judd, L. M., Noonan, W. T., Andringa, A., Doetschman, T., Manning, P. A., Liu, L. H., Miller, M. L., and Shull, G. E. (2002) *J. Biol. Chem.* **277,** 37871–37880
48. Hartner, A., Cordasic, N., Klanke, B., Veelken, R., and Hilgers, K. F. (2003) *Nephrol. Dial. Transplant.* **18,** 1999–2004
49. Sontia, B., Montezano, A. C., Paravicini, T., Tabet, F., and Touyz, R. M. (2008) *Hypertension* **51,** 915–921
50. Heitzmann, D., Derand, R., Jungbauer, S., Bandulik, S., Sterner, C., Schweda, F., El Wakil, A., Lalli, E., Guy, N., Mengual, R., Reichold, M., Tegtmeier, I., Bendahhou, S., Gomez-Sanchez, C. E., Aller, M. I., Wisden, W., Weber, A., Lesage, F., Warth, R., and Barhanin, J. (2008) *EMBO J.* **27,** 179–187
51. Hoeflich, A., and Bielohuby, M. (2009) *J. Mol. Endocrinol.* **42,** 191–203
52. Ferreira, J. G., Cruz, C. D., Neves, D., and Pignatelli, D. (2007) *J. Endocrinol.* **192,** 647–658
53. John, M. E., John, M. C., Boggaram, V., Simpson, E. R., and Waterman, M. R. (1986) *Proc. Natl. Acad. Sci. U.S.A.* **83,** 4715–4719
54. Hanukoglu, I., Feuchtwanger, R., and Hanukoglu, A. (1990) *J. Biol. Chem.* **265,** 20602–20608
55. Waterman, M. R., and Simpson, E. R. (1989) *Recent Prog. Horm. Res.* **45,** 533–563
56. Quinn, S. J., and Williams, G. H. (1988) *Annu. Rev. Physiol.* **50,** 409–426
57. Groenink, L., Dirks, A., Verdouw, P. M., Schipholt, M., Veening, J. G., van der Gugten, J., and Olivier, B. (2002) *Biol. Psychiatry* **51,** 875–881
58. Stenzel-Poore, M. P., Cameron, V. A., Vaughan, J., Sawchenko, P. E., and Vale, W. (1992) *Endocrinology* **130,** 3378–3386
59. Dirks, A., Groenink, L., Bouwknecht, J. A., Hijzen, T. H., Van Der Gugten, J., Ronken, E., Verbeek, J. S., Veening, J. G., Dederen, P. J., Korosi, A., Schoolderman, L. F., Roubos, E. W., and Olivier, B. (2002) *Eur. J. Neurosci.* **16,** 1751–1760
60. Stenzel-Poore, M. P., Heinrichs, S. C., Rivest, S., Koob, G. F., and Vale, W. W. (1994) *J. Neurosci.* **14,** 2579–2584
61. van Gaalen, M. M., Stenzel-Poore, M. P., Holsboer, F., and Steckler, T. (2002) *Eur. J. Neurosci.* **15,** 2007–2015
62. Timpl, P., Spanagel, R., Sillaber, I., Kresse, A., Reul, J. M., Stalla, G. K., Blanquet, V., Steckler, T., Holsboer, F., and Wurst, W. (1998) *Nat. Genet.* **19,** 162–166
63. Welch, J. M., Lu, J., Rodriguiz, R. M., Trotta, N. C., Peca, J., Ding, J. D., Feliciano, C., Chen, M., Adams, J. P., Luo, J., Dudek, S. M., Weinberg, R. J., Calakos, N., Wetsel, W. C., and Feng, G. (2007) *Nature* **448,** 894–900
64. Horton, W. A., Hall, J. G., and Hecht, J. T. (2007) *Lancet* **370,** 162–172